DIAGNOSTICS FOR INTENSE HEAVY ION BEAMS IN THE HIF-VNL*

F. M. Bieniosek†, S. Eylon†, A. Faltens†, A. Friedman‡, J.W. Kwan†, M.A. Leitner†, A.W. Molvik‡, L. Prost†, P.K. Roy†, P.A. Seidl†, G. Westenskow‡

†Lawrence Berkeley National Laboratory, Berkeley, CA, USA and HIF-VNL

‡Lawrence Livermore National Laboratory, Livermore, CA, USA and HIF-VNL

Abstract

Modern diagnostic techniques provide detailed information on beam conditions in injector, transport, and final focus experiments in the HIF-VNL. Parameters of interest include beam current, beam energy, transverse and longitudinal distributions, emittance, and space charge neutralization. Imaging techniques, based on kapton films and optical scintillators, complement and in some cases, may replace conventional techniques based on slit scans. Time-resolved optical diagnostics that provide 4-D transverse information on the experimental beams are in operation on the existing experiments. Current work includes a compact optical diagnostic suitable for insertion in transport lines, improved algorithms for optical data analysis and interpretation, a high-resolution electrostatic energy analyzer, and an electron beam probe. A longitudinal diagnostic kicker generates longitudinal space-charge waves that travel on the beam. Time of flight of the space charge waves and an electrostatic energy analyzer provide an absolute measure of the beam energy. Special diagnostics to detect secondary electrons and gases desorbed from the wall have been developed.

---

*This work performed under the auspices of the U.S Department of Energy by University of California, Lawrence Livermore and Lawrence Berkeley National Laboratories under contracts No. W-7405-Eng-48 and DE-AC03-76SF00098.

Corresponding author:
Frank Bieniosek
Lawrence Berkeley National Laboratory
1 Cyclotron Road Bldg 47R0112
Berkeley, CA, 94720-8201 USA
Tel: 510-486-4245
Fax: 510-486-5392
Email: fmbieniosek@lbl.gov

PACS Codes: 52.59.Sa, 52.70Nc, 52.70Kz, 29.30.Aj, 41.75.Ak, 41.85.Qg
Keywords : inertial fusion energy, heavy ion beam, linear accelerator, space-charge, phase space, diagnostics

Introduction

This paper provides an overview of recent diagnostic development in the HIF-VNL, and a brief discussion of expected trends in diagnostic requirements. The beams in current HIF-VNL experiments range in energy from 50 keV to 2 MeV, with current densities from <1 to >100 mA/cm^2, and pulse lengths of 4 to 20 μs. Beam ions include the alkali ions K^+ and Cs^+ produced in surface ionization sources, and ions such as Ar^+ from gas sources. These beams are generally space-charge dominated, with high transverse fill factors. Diagnostic access is limited by high longitudinal occupancy in beam transport lines. High quality diagnostic data is essential to maximize experimental productivity, and in view of the heavy reliance placed on simulation in the HIF development path.

In this paper the diagnostics are grouped into three categories.

1. Intercepting. These include Faraday cups, slit (emittance) scanners, kapton and optical imaging, electrostatic energy analyzer, and detectors that measure halo and beam-wall interactions.
2. Passive nonintercepting. These include magnetic and capacitive pickups, secondary particle diagnostics, and optical emission spectroscopy.
3. Active nonintercepting. These include particle beam probes and diagnostics utilizing externally generated space charge waves.

1. Intercepting

Intercepting diagnostics physically place a solid material object in the path of the beam. Since the range of heavy-ion beams at the energy of present-day HIF-VNL experiments is very short (~1 μm), only the thinnest foils do not stop the beam entirely. Copious amounts of secondary electrons (≥10 electrons per ion) and a cloud of gas (≥1000 desorbed gas atoms per incident beam ion) are generated by the incident beam as it strikes the intercepting surface. It is often necessary to trap secondary electrons by a potential barrier or to sweep out electrons from the beam by clearing fields to prevent seriously affecting beam dynamics.

A Faraday cup to measure heavy ion beam current generally consists of a shielded, negatively biased electron suppressor, and a deep, positively biased ion collector. Large Faraday cups intercept the entire beam. Charged particles from the gas cloud generated at the surface of the ion collector may interfere with the measurement unless they are carefully suppressed by a mesh or honeycomb material on the collector surface and strong electron suppressor voltages.

A 32-channel array of small Faraday cups (FCA) was used to characterize the beam distribution in the 2-MV Injector diode [1]. It consists of an array of small Faraday cups (1-mm diameter entrance aperture) arranged in two orthogonal rows mounted in a single movable assembly. The collectors are staggered in radius with a center to center separation of 3.8 mm. The assembly can be rotated and moved along the beam axis. Figure 1 shows the configuration of the collectors on the FCA. Great care was taken to align the array, to suppress plasma and gas cloud formation, and to ensure uniform response of the device by designing and biasing the detectors such that the collected signal does not depend on secondary electron emission, which is sensitive to details of surface conditions of each detector surface. Figure 2 shows a beam profile derived from the FCA diagnostic.

Transverse slit scanners consist of pairs of independently-driven paddles (horizontal or vertical) each holding a slit or slit-cup (a compact assembly composed of a shallow Faraday cup or simple collector plate behind a masking slit). Slits are typically 50-100 μm wide. These scanners are commonly operated in several configurations: a single slit-cup measures 1-dimensional beam profiles; slit/slit-cup scanners measure the two-dimensional transverse f(x,x′,t), f(y,y′,t) phase space and emittance of the beam; and crossed-slit arrangements (e.g. a vertical slit paired with a horizontal slit-cup) measure the 2-dimensional beam distribution f(x,y,t). Careful slit-to-slit alignment is necessary for accurate phase space measurements. The angular resolution requirement is <0.5 mrad. The width of the slits and the drift distance between the slit and slit-cup are determined by considerations of beam temperature and space charge. Slit-cups may be biased to eject secondary electrons to amplify the collected ion signal. In order to build up a complete scan of the beam, these devices depend on pulse-to-pulse reproducibility of the beam properties over many beam pulses (tens of pulses for 1-D scans, to thousands of pulses for crossed-slit scans). However it is possible to reduce the data acquisition time by introducing multiple slits or slit-cups. Time resolution is excellent.

Imaging of the beam on kapton film [3] is effective in the energy range ~0.05 to >2 MeV. Ion-beam induced darkening of the film provides a direct measure of the time-integrated beam intensity profile. Kapton has excellent spatial resolution and discrimination against stray low mass and low energy particles. Kapton requires ~100 beam pulses to form a usable image. A kapton image of the beam in the HCX [2] is shown in Figure 3. Because of the lack of time resolution, utility of kapton is limited by its sensitivity to the rapidly varying head and tail of the beam pulse.

Optical imagers [4] are an area of growing interest because of their ability to rapidly provide high quality time-resolved 4-dimensional information about the intercepted beam. We have developed techniques for imaging beams using ceramic (96% Al_2O_3) scintillator material imaged by a fast, image-intensified CCD camera (Roper Scientific). Inorganic scintillators are widely used as beam profile monitors, and the mechanism and optical response to an ion beam have been studied extensively [5]. Charge neutralization is provided by a high-transparency metallic

mesh placed on or near the surface of the scintillator. Beam ions striking the mesh provide sufficient secondary electrons to charge-neutralize the insulating scintillator surface. Light emitted from the thin (0.1 mm) wafer of alumina may be imaged from the front or rear. The measured rise time of the scintillator is <50 ns. The fall time is more complicated, with most of the optical signal decaying on a ≤1 μs time scale. The lifetime of the scintillator material is limited under intense ion beam bombardment. For an HCX K^+ beam (kinetic energy = 1.0 MeV, pulse length = 4 μs, current density = 60 mA/cm^2) the optical emission decays with an e-folding rate of ~170 beam pulses. As a result, for intense beams it is helpful to limit intensity by placing holes or slits upstream of the scintillator. There is no evidence for saturation or thermal quenching when the beam intensity is reduced in this manner.

In addition to the usual 2-dimensional beam distributions provided by slit scanners, optical diagnostics have the capability to image the beam in all four transverse dimensions. By interposing horizontal and vertical slits, phase space projections (f(x,y,y′), f(x,x′,y) are measured; and with an array of pinholes, the full distribution f(x,x′,y,y′) is measured. Figure 4 shows the arrangement of an optical slit scanner.

In a compact folded arrangement (Fig. 5), the beam image is viewed from the front of the scintillator through a mirror. This arrangement adds complexity to the optical system and to the task of unfolding the image because of the variation in optical path length across the image. However, it reduces the longitudinal space required by the diagnostic to a minimum, a necessary feature to diagnose the beam in a transport experiment with high longitudinal occupancy such as HCX. Resolution is determined by the drift distance between the slit and the scintillator, the camera optics and the camera CCD array size.

Figure 6 shows a series of beam images in the scintillator for a slit at various horizontal locations across the HCX beam, and a pinhole image, which provides information on f(x′,y′) at the location of the pinhole. By integrating the images along the long dimension, the image data may be processed in the same manner as double-slit scanner data for the same beam. A comparison of results from the two diagnostics for the same beam yields agreement with the double-slit scanner data for beam size and angle [4], but increased noise in the optical image signal compared to the double-slit scanner is reflected in a higher determination of the emittance. The hooking at the top and bottom of the slit images represent a nonuniformity or distortion in the horizontal particle distribution x′ such that x′ is a function of not only x but also y. This distortion broadens the line integrated profile as measured by the double-slit scanner, and illustrates the limitations to synthesizing the 4-D beam particle distribution from the double-slit scanner data alone.

A reconstructed image is shown in Fig. 7a. This profile was developed from an optical slit scan (as in Figure 6) using 31 HCX beam pulses. It represents the transverse beam intensity distribution referred to the horizontal slit plane. The assumption of a linear transformation of the beam between the slit and the screen is made. Figure 7b shows the equivalent

profile of the beam constructed by building up an image point-by-point using a pair of crossed slits. This image required 4096 beam pulses. Similar images of the moments of the beam distribution, and the local RMS angle spread (which is related to the transverse beam temperature distribution), are also constructed from the optical data.

Algorithms for reconstruction of the beam profiles in all transverse dimensions have been developed [6]. Figure 8 shows the beam for two rotation angles in x-y-x' space.

Quantitative interpretation of the images may be affected by other factors. Since the scintillator is sensitive to energetic charged particles, such as electrons, it should be biased to not attract energetic electrons. In addition, there is an optical signal from beam interaction with ambient gas, including the gas cloud that is created at a wall when bombarded by the intense ion beam. Images taken through a hole plate show optical signal attributed to this effect through the holes that can be significant for intense or tightly-focused beams. This effect can also be expected to occur at the front surface of the scintillator, resulting in an additional contribution to the light output from the surface of the scintillator that is proportional to the product of the beam intensity and the local density of the gas cloud at the surface. This contribution may be significant in the case of tightly-focused beams, and the relative contribution of this signal to the total light signal is being investigated.

The optical signal from beam interaction with ambient gas provides an alternate imaging technique that is rugged and self-healing. It may prove to be a useful remote diagnostic of beam-wall interactions, and for nonintercepting diagnostics of beam transport by interaction with ambient or injected gas.

Interpretation of the results from all intercepting diagnostics of transverse velocity components (x′,y′) should include the effect of the conducting slit plate, which shorts out the self-field of the beam over a distance similar to the transverse beam dimension. For beams with significant space charge, this effect systematically changes the apparent beam divergence angle by ~1 mrad, a significant effect for detailed comparisons with theoretical models.

An electrostatic energy analyzer (EEA) is used to measure the beam energy and beam energy distribution. We have used cylindrical 90-degree-bend analyzers with first order focus [7] to measure the time evolution of the mean beam energy in HCX [2] and the rate of charge exchange of beam ions in a gas source on STS-100 [8]. In addition to its utility as an energy analyzer, the EEA can also be used to discriminate and analyze beam ions that have been doubly ionized by interaction with ambient gas. This property can be used as a direct probe of beam-gas and beam-wall interaction.

An energy analyzer (Fig. 9) with improved energy resolution is under design. Improved energy resolution provides improved information on the longitudinal beam distribution $f(p, \Delta p/p)$. Thus, in combination with optical diagnostics, information on all 6 dimensions in beam phase space becomes available. Improved understanding of beam energy spread is important for drift compression experiments, increased sensitivity to

charge exchange and processes such as temperature anisotropy instability, to study and correct energy errors in the head and tail of the beam pulse, beam energy ripples, and longitudinal space charge waves. The goal is to achieve energy resolution $\Delta E/E \sim 10^{-4}$. Careful attention must be paid to mechanical tolerance and alignment, stability of HV supplies, fringe fields, space-charge effects, and beam/plasma loading.

II. **Passive nonintercepting**

The insertion of a physical diagnostic into the path of the beam inevitably leads to secondary effects such as gas clouds, secondary electron emission, and shorting out of the beam's self electric fields. At higher intensities the role of diagnostics becomes more challenging as these secondary effects become increasingly difficult to overcome, and diagnostic apparatus becomes subject to damage by the intense beams. As a result nonintercepting diagnostics are of great interest.

A magnetic current monitor (or Rogowski coil) consists of a coil that is shielded from beam ions and wound around an air or iron core [9]. It acts as a current transformer to measure the magnetic field induced by the beam current threading the coil. Because electrons streaming with or against the beam affect the measured current, an electron suppressor is necessary.

Segmented capacitive probes have been developed to measure the transverse position of the beam as a function of time [10]. The electrostatic quadrupoles (ESQs) in an electrostatic transport section, such as on HCX, have been instrumented. A capacitively induced current spike the head and tail of the beam passing through the ESQs. In addition collected charge on the ESQs provides information on secondary particles due to interactions of the beam with residual gas and beam losses due to scraping [2].

Secondary particles are those particles ejected by the beam from the wall or from the vicinity of the beam after interaction with the background gas. Techniques for instrumenting the wall to measure secondary particles and beam-wall interactions have been developed [11]. These include an instrumented target to measure gas evolution and secondary electron production at a wall as a function of angle of incidence. Gridded and flush probes located at the wall are designed to measure electron emission and gas desorption by collecting and measuring the flux of secondary particles at the wall. A gridded ion energy analyzer for example can measure the energy of particles expelled from the beam and thus in principle the potential of the beam.

III **Active nonintercepting**

The electron beam probe (EBP) [12, 13] is a low current ~1-10 μA, ~5-10 keV electron beam injected transversely across the path of the ion beam to be probed. The deflection of the probing electron beam in the field of the ion beam provides information about the space-charge distribution, while leaving the ion beam unchanged. The electron beam is injected in a plane perpendicular to the ion beam on a path that may be varied from pulse to pulse to probe the

entire cross section of the ion beam. Electrons are detected on a scintillator plate placed on the other side of the ion beam. The deflection of the electron beam as a function of initial position may be inverted to determine the line-integrated charge density of the ion beam under the assumption of cylindrical symmetry. The EBP is sensitive to both radial and longitudinal electric fields in the ion beam, and time resolution is provided by a blanking pulse train applied to the electron gun. The diagnostic provides information on the degree of local space charge neutralization of the ion beam by trapped electrons. Space charge neutralization is an important parameter in transport, beam compression, and final focus. An EBP has been installed on the NTX experiment [13].

Longitudinal diagnostic kickers have been installed on both HCX and NTX to generate space charge waves [14, 15]. The space-charge waves are longitudinal oscillations of the beam within a conducting wall. These waves travel downstream with the beam and are collected at a diagnostic end station. To describe the space-charge waves we apply the one-dimensional fluid equations. A relatively short-duration, small amplitude (~1% in beam energy) energy perturbation is applied to the beam using a specially designed fast pulser. These energy pulses manifest as beam current perturbations, about 10% in amplitude when measured a few meters downstream. One valuable application of these waves is the measurement of the beam energy by time of flight

Projected developments

The recent trend has been toward increasing reliance on optical diagnostics that provide large amounts of detailed information on the beam particle distribution. Further technical improvements are required to improve reliability and utility of quantitative measurements using the optical diagnostics, including software for image processing and data analysis to integrate the experiments more closely with detailed beam simulations.

Projected HIF-VNL experiments will have higher beam energy density and shorter pulses, with greater reliance on plasma focusing schemes, such as in neutralized drift compression. Under these conditions, intercepting diagnostics will be increasingly less desirable as they perturb the neutralizing plasma. Greater emphasis will be on diagnostics that are faster, nonintercepting, and compatible with plasma, some of which are now under development, and some of which have not yet been developed. Other projected areas of emphasis include diagnostics to study halo formation and growth, and to study longitudinal beam dynamics.

REFERENCES

1. FM Bieniosek, E Henestroza, JW Kwan, L Prost, P Seidl, 2-MV Injector for HCX, Proc. of Particle Accelerator Conference, Chicago, IL June 18-22, 2001, p. 2099.
2. L Prost, FM Bieniosek, CM Celata, CC Dugan, A Faltens, PA Seidl, WL Waldron, R Cohen, A Friedman, M Kireeff Covo, SM Lund, AW Molvik, Experimental study of the transport limits of intense heavy ion beams in the HCX, these proceedings.
3. FM Bieniosek, JW Kwan, L Prost, PA Seidl, Imaging of heavy-ion beams on kapton film, Rev Sci Instrum 73, 2867 (2002).
4. FM Bieniosek, L Prost, W Ghiorso, Beam imaging diagnostics for heavy ion beam fusion experiments, Proc. of Particle accelerator Conference, Portland, OR, May 12-16, 2003, p. 2524.
5. RB Murray and A Meyer, Scintillation response of activated crystals to various charged particles, Phys. Rev. 122, 815 (1961).
6. A Friedman, FM Bieniosek, CM Celata, DP Grote, LR Prost, PA Seidl, Simulations using initial 4D beam particle distributions synthesized from experimental data, Proc. of Particle accelerator Conference, Portland, OR, May 12-16, 2003, p. 275.
7. RE Warren, JL Powell, RG Herb, Electrostatic analyzer for selection of homogenous ion beam, Rev. Sci. Instrum. 18, 559 (1947).
8. GA Westenskow, DP Grote, E Halaxa, JW Kwan, J Kapica, WL Waldron, RF Plasma source for heavy ion fusion, these proceedings.
9. DG Pellinen, MS Di Capua, SE Sampayan, H Gerbracht, M Wang, Rogowski coil for measuring fast, high-level pulsed currents, Rev. Sci. Instrum. 51, 1535 (1980).
10. FJ Deadrick, JJ Barnard, TJ Fessenden, JW Meridith, J Rintamaki, Development of beam position monitors for heavy ion recirculators, Proc. of Particle Accelerator Conference, Dallas TX, May 1995, 2557 (1995).
11. AW Molvik, RH Cohen, A Friedman, M Kireeff Covo, SM Lund, G Westenskow, FM Bieniosek, S Eylon, A Faltens, E Henestroza, JW Kwan, L Prost, PK Roy, PA Seidl, JL Vay, S Yu, Experimental studies of electrons in a heavy-ion beam, these proceedings.
12. J Shiloh, M Lampel, R Sah, Electron beam probe for charge neutralization studies of heavy ion beams, RSI 54, 46 (1983).
13. PK Roy, SS Yu, S Eylon, E Henestroza, J Ludvig, DB Shuman, WG Greenway, DL Vanecek, WL Waldron, R Hannink, Study of a non intercepting ion beam diagnostic for beam density profile, these proceedings.
14. M Reiser, Theory and design of charged particle beams, Wiley Interscience, New York, 1994.

15. FM Bieniosek, A Faltens, L Prost, PK Roy, PA Seidl, S Eylon, E Henestroza, W Waldron, SS Yu, Experimental study of space-charge waves in intense heavy ion beams, these proceedings.

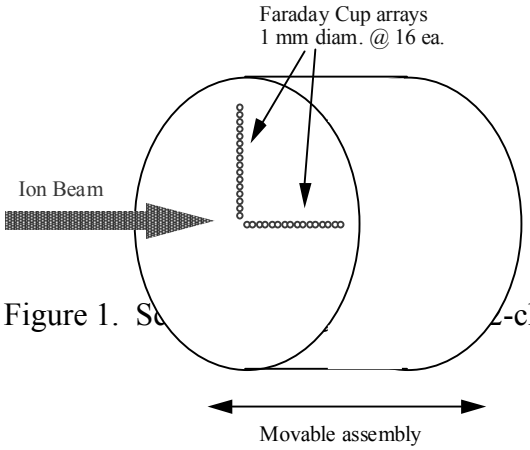

Figure 1. Sc -channel Faraday cup array.

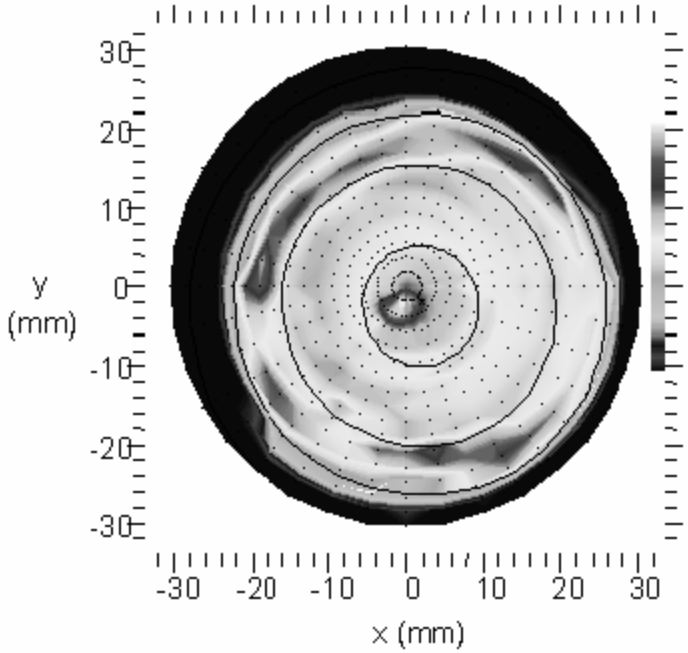

Figure 2. Contour map of the beam current density profile at the exit of the diode of the 2 MV Injector.

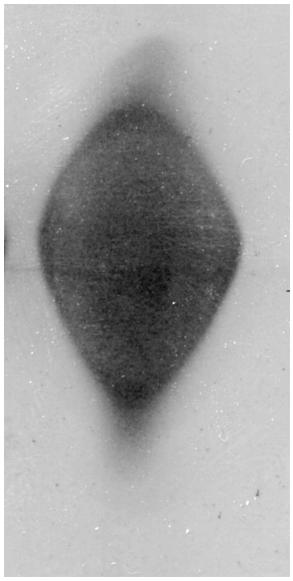

Figure 3. A kapton image of the beam in HCX, showing the characteristic diamond shape. The kapton film was exposed for 40 beam pulses. The smearing at the top and bottom of the image is due to the head and tail of the beam pulse.

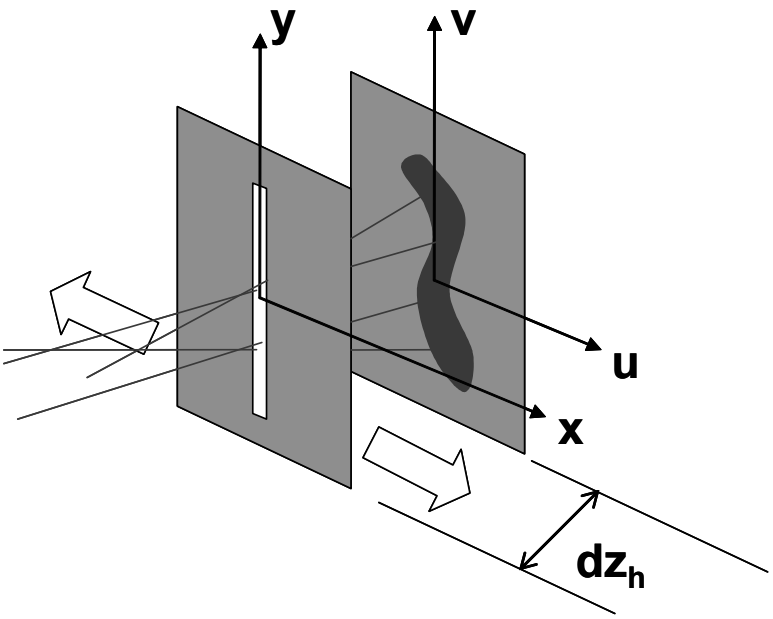

Fig 4. Schematic of the optical slit scanner. The beam ions passing through the first slit produce an image on the scintillator that provides information on their transverse velocity. The technique for converting the information in the scintillator plane (u,v) to beam properties at the slit plane (x,y) is described in Ref. 6.

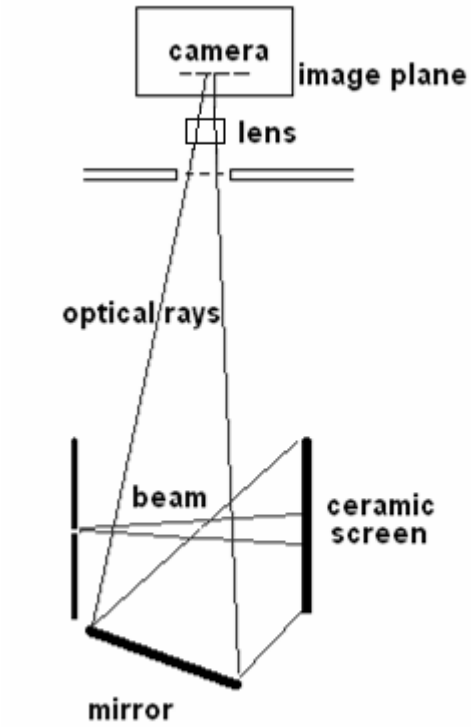

Fig. 5. Compact folded optical slit scanner. The beam passes through the entrance slit or pinholes on the left, and creates an image on the ceramic scintillator screen at right. The camera views the image through a mirror.

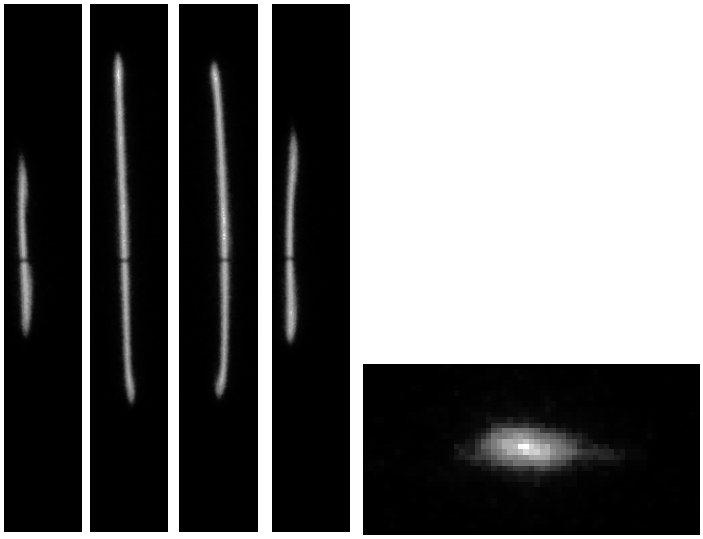

Fig. 6. A series of slit image and a pinhole image from HCX.

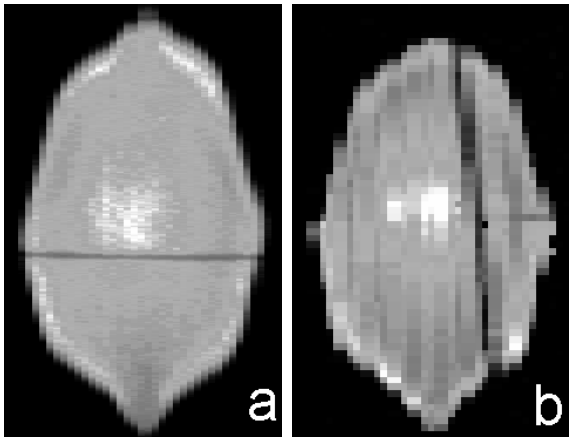

Fig. 7. Constructed image of the HCX beam intensity profile based on measured (a) optical slit scan and (b) mechanical crossed-slit measurement. The scale for both images is 3.0 x 4.68 cm.

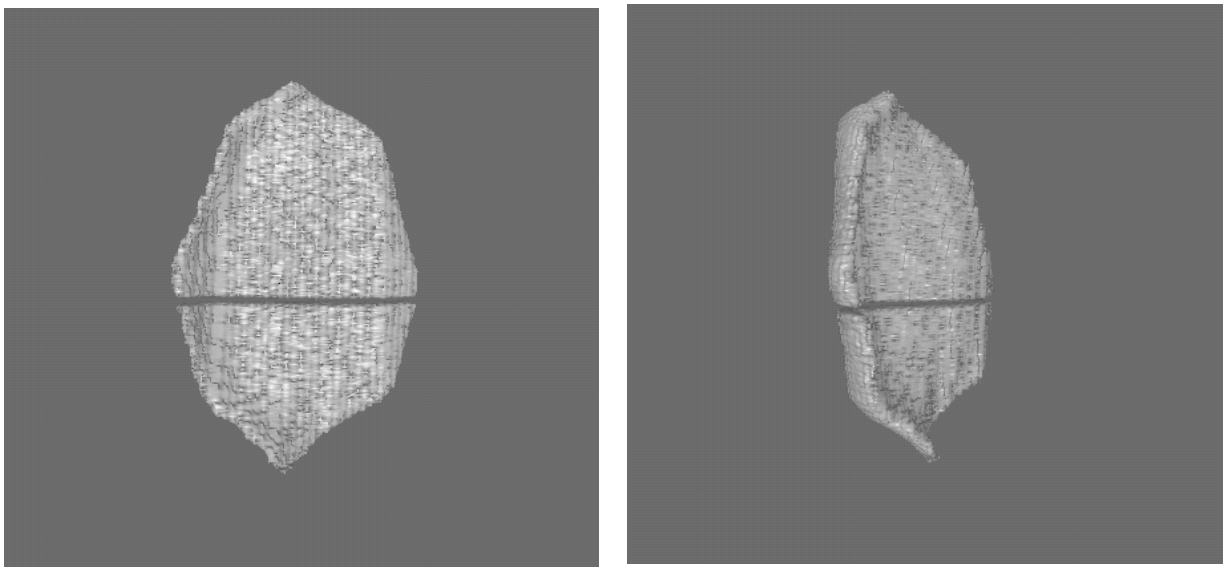

Fig 8. Isosurface where f(x,y,x′)=30% of peak.

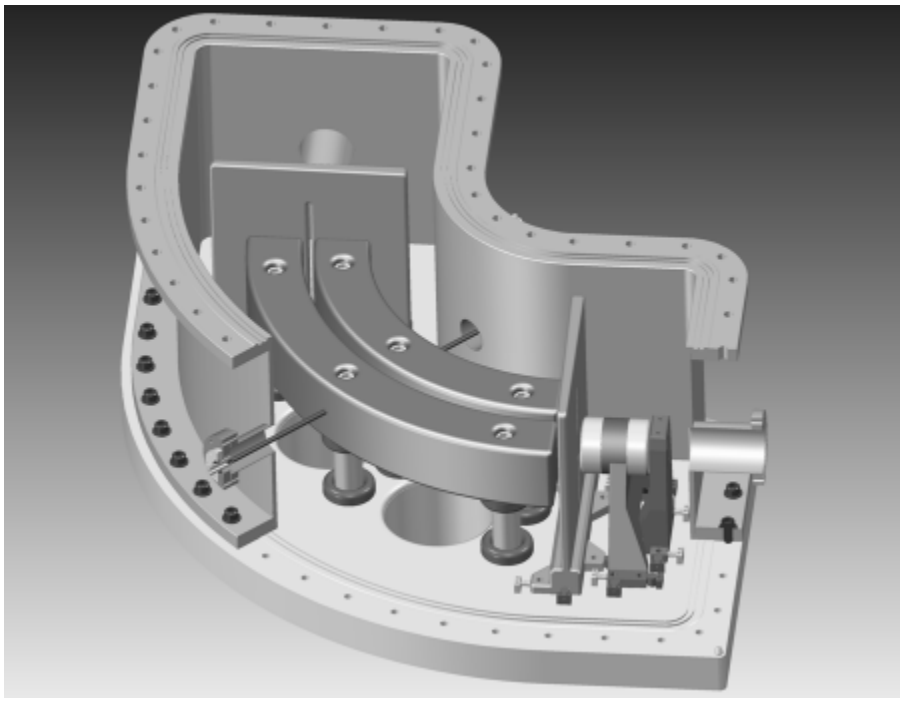

Fig 9. Plan view of the electrostatic energy analyzer under design. The beam enters through an entrance slit at bottom right. It is deflected through an angle of 90 degrees by the curved analyzer plates and imaged on a detector located at top left. The radius of curvature is 0.5 m.